Reconnaissance assessments of three contractional fault-related folds along the Quebradas Back Country Byway, Socorro County, New Mexico

Stephen C. Hook and Peter A. Brennan
2022, pp. 305-319. https://doi.org/10.56577/FFC-72.305

in:

Socorro Region III, Koning, Daniel J.; Hobbs, Kevin J.; Phillips, Fred M.; Nelson, W. John; Cather, Steven M.; Jakle, Anne C.; Van Der Werff, Brittney, New Mexico Geological Society 72nd Annual Fall Field Conference Guidebook, 426 p. https://doi.org/10.56577/FFC-72

This page is intentionally left blank to maintain order of facing pages.

New Mexico Geological Society Guidebook, 72nd Fall Field Conference, 2022, p. 305–319.

RECONNAISSANCE ASSESSMENTS OF THREE CONTRACTIONAL FAULT-RELATED FOLDS ALONG THE QUEBRADAS BACK COUNTRY BYWAY, SOCORRO COUNTY, NEW MEXICO

STEPHEN C. HOOK[1] AND PETER A. BRENNAN[2]

[1]Atarque Geologic Consulting, LLC, 411 Eaton Avenue, Socorro, NM 87801; bellaplicata@gmail.com
[2]Tellumetrics, LLC, 5003 Plantation Colony Court, Sugar Land, TX 77478

Abstract—Contractional kink folds developed in Paleozoic strata along the Quebradas Back Country Byway, Socorro County, New Mexico, are interpreted using pattern recognition as simple fault-bend and simple-step fault-propagation folds with easterly slip. These fold types are present at outcrop scale (<30 m across and a few meters of structural relief) to sub-regional scale (>5 km along strike and >10 m of structural relief) along the Byway. Cross sections of the folds are exposed along canyon walls and in hillsides. These interpretations imply that the folds developed above bends in nonplanar, low-angle thrust faults in individual thrust sheets and did not originate along high-angle reverse faults at great depth.

A simple fault-bend fold is a balanced, geometric model of deformation in which the causative fault is throughgoing, steps up from a lower detachment to an upper detachment, and has a flat-ramp-flat geometry, above which an open, roughly symmetrical fold with relatively gently dipping limbs is developed; more slip enters than exits the fold; and the front limb is steeper and shorter than the back limb. A simple-step fault-propagation fold is a balanced, geometric model of deformation in which the fault steps up from a bedding-parallel detachment and has a flat-ramp geometry: a closed, asymmetrical fold with a short, steep to overturned front limb and a longer, more gently dipping back limb lies above the ramp. In initial stages, no slip exits the fold, bed offset decreases to zero upward along the fault, the front synclinal axis terminates at the fault tip, and folding occurs at the fault tip located in the core of the fold.

NMGS Field Trip Stop #2 (Day 1) offers a great example of an outcrop-scale, cross-sectional view of folds and faults that developed in Permian strata near the southern end of the Byway. This outcrop (called Fold #1 in this paper) contains a complex mixture of many of the structural styles present in the Quebradas region: faults range from low-angle, Laramide thrust faults to a high-angle, Neogene normal fault; contractional folds include a fault-propagation fold and fault-bend folds. Most of the faults have <2 m of displacement. Folds have developed only above bends in thrust faults comprised of nonplanar segments or at the tip line of a thrust fault. Offset of beds along planar faults was by rigid block translation; the lack of fault-plane bends resulted in beds being moved up or down the faults without dip change or drag. Fold #1 exhibits many of the characteristics of a simple-step fault-propagation fold.

NMGS Field Trip Stop #3 (Day 1) is in the Tajo structural zone, which developed in Pennsylvanian and Permian strata near the middle of the Quebradas region. Fold #2 is a large anticline developed in Pennsylvanian strata that has a steep, highly overturned front limb and a long, planar back limb with a well-defined back syncline. The fold's causative fault is not exposed. Based on fold-shape parameters, we interpret this structure as a fault-propagation fold whose causative fault stepped up easterly at ~15° from a detachment. Slip on this fault created a large fault-propagation fold with an overturned front limb. The fold was unable to grow self-similarly as slip increased, and the fault broke through the fold along a zone of weakness below its anticlinal axis. Our interpretation is illustrated by a generic fault-propagation fold model with high-angle breakthrough.

Fold #3 (included in Day 1 Field Trip Stop #3) is an outcrop-scale, kink fold with a slightly overturned front limb developed in Permian strata in front of—to the east of—the Tajo folds. This small kink fold is preserved as a breached anticline-syncline pair. The planar back limb and back syncline of the fold form a conical hill capped by resistant gray carbonate strata. The back limb dips ~28°W. The crest of the fold and upper part of the front limb are eroded, but two thin, slightly overturned sandstone beds in the valley to the east of the hill correlate to the two resistant sandstone beds in the back limb. The reconstructed fold pattern is typical of the core of a classic fault-propagation fold.

Bed thickness is conserved in these folds, which are interpreted to have developed through bedding-plane slip and kink-band migration in the brittle domain. Folding did not involve gypsum or ductile deformation. All assessments are presented as first-order, reconnaissance interpretations that are intended to provide an alternative approach to the published understanding of the complex structural geology of the Quebradas region. These assessments are not all inclusive and should be supplemented with geologic map observations and related interpretations.

INTRODUCTION

Cather and Koning (in press) have designated a rectangular area ~5 km east of Socorro, New Mexico, as the Quebradas region (Fig. 1). This region is a structurally complex area that extends ~17 km north-south and ~28 km east-west. It consists of the following six contiguous 7.5-minute geologic quadrangles: (1) Mesa del Yeso (Cather et al., 2004); (2) Sierra de la Cruz (Cather et al., 2012); (3) Loma de las Cañas (Cather and Colpitts, 2005); (4) Bustos Well (Cather et al., 2014); (5) San Antonio (Cather, 2002); and (6) Cañon Agua Buena (Cather et al., 2007).

Details of the geologic history and stratigraphy of this area can be found in Cather and Koning (in press), papers in the guidebook (Lucas et al., this volume (a) and (b); Dietz and McLemore, this volume), and in each of the six geologic quadrangle maps that comprise the region. The Quebradas region consists of ~1400 m thick succession of Pennsylvanian and Permian strata that overlies Proterozoic granite. In ascending order, Pennsylvanian strata include the Sandia Formation (sandstone, shale, minor conglomerate, minor limestone), Gray Mesa Formation (mostly limestone and shale), and the Atrasado Formation (shale, limestone, sandstone). Overlying a transitional unit (25–120 m thick Bursum Formation), the

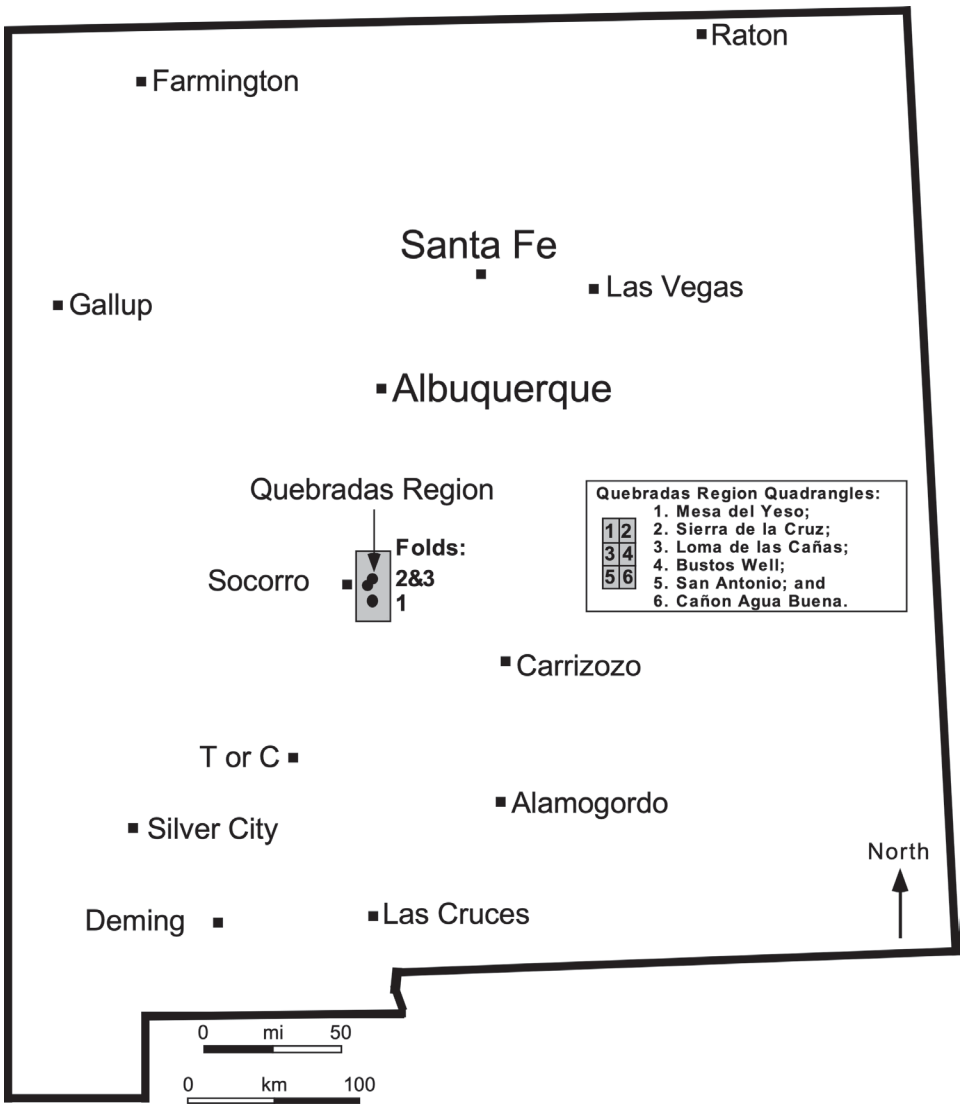

FIGURE 1. Map of New Mexico showing the Quebradas region east of Socorro and the approximate locations of the three outcrops discussed in the text. The Quebradas region is comprised of the six contiguous 7.5-minute quadrangle maps listed in the inset.

lower ~300 m of the Permian is characterized by red beds of the Abo Formation overlain by the Meseta Blanca Formation of the Yeso Group (Arroyo de Alamillo Formation *sensu* Lucas et al., 2005); both of these formations are composed mainly of siltstone, mudstone, and sandstone. The next overlying unit germane to our study is the Torres Member of the Los Vallos Formation (Yeso Group), which is ~160 m thick and composed of siltstone, claystone, gypsum, and a few, prominent beds of carbonates (primarily dolomites). The remaining members of the Los Vallos Formation and the overlying, Permian-age Glorieta and San Andres formations lie above the studied exposures in our paper and total ~290 m. These strata have been folded and faulted by three tectonic events (Cather and Axen, in press). The Laramide orogeny created west-up, reverse, and thrust faults and associated folds as well as dextral strike-slip faults; these structural elements extend from Torrance County on the north southwards into Sierra County, parallel to the present-day eastern boundary of the Rio Grande Valley. During a poorly time-constrained interval within ~45–20 Ma, regional, km-scale displacement occurred along the Quebradas detachment fault system. Later Rio Grande rift tectonism (25–0 Ma) resulted in a plethora of normal faults and variable domains of stratal tilts.

Most of the Quebradas region is traversed by a 39 km long (24 mi long), north-south dirt road that is part of the U.S. Bureau of Land Management's National Scenic Byways Program. This road, the Quebradas Back Country Byway, can be accessed from the major, paved highways in the area: U.S. Interstate 25 to the west or U.S. Highway 380 to the south (Scholle, 2010). The Quebradas region is the primary focus of Day 1 of the New Mexico Geological Society's 2022 Fall Field Conference (Koning et al., this volume). A free guidebook for laymen to the geology of the area (Scholle, 2010) is available from the New Mexico Bureau of Geology and Mineral Resources and the Bureau of Land Management.

Compressional kink folds with easterly tectonic transport are common in the complexly folded and faulted Paleozoic strata that crop out along the Byway primarily near the center of the Quebradas region (e.g., Cather and Colpitts, 2005). These folds formed during the Laramide and have been overprinted by Neogene normal faulting (Cather and Axen, in press). These kink folds range from outcrop scale (<30 m across and a few meters of structural relief) to sub-regional scale (>5 km along strike and >10 m of structural relief). The folds consist of relatively long, planar limb-segments with homogeneous dips that change dip abruptly at axial surfaces. This folded belt has been called the "Tajo folds" by Cather and Colpitts (2005) and the "Tajo structural zone" by Cather and Axen (in press). These kink folds have been identified as fault-bend and fault-propagation folds by Cather and Colpitts (2005), Scholle (2010), and Cather and Axen (in press), but these sources have not provided descriptions of the geometry or kinematic development of the structures. We interpret folds from three areas in the Quebradas region as either fault-bend or fault-propagation folds and explore the geologic implications of these first-order interpretations.

We have neither mapped the rocks nor measured any sections of Paleozoic strata in the Quebradas region. For this information, we have relied on published or furnished resources. Without knowing the thicknesses of all the rock units, it is not possible to make definitive cross sections of the folds. Therefore, we present balanced models of generalized fault-related folds as first-order interpretations. Fault-bend-fold theory, developed by Suppe (1983, 1985), is a two-dimensional, geometric and kinematic approximation of three-dimensional folds in which folding takes place when strata are translated across bends in nonplanar fault segments. Fault-propagation fold theory (Suppe, 1985; Suppe and Medwedeff, 1990) is a two-dimensional, geometric and kinematic approximation in which folding takes place in front of a propagating fault surface. The assumptions common to both theories are that (1) stratal thickness, (2) cross-sectional area, and, therefore, (3) bed line length are conserved during the folding process. Folding occurs primarily by kink-band migration as zones of homogeneous dip (bounded by paired axial surfaces) grow and move with increasing fault slip. All fold models are geometrically balanced but may not be geologically correct. For a model to be balanced, a "before-folding" and an "after-folding" comparison must demonstrate conservation of thickness, area, and line length.

The presence of oblique slip in the Tajo structural zone (Gary Axen, pers. commun., 2022) complicates balanced cross section construction. Therefore, we present only balanced models of the folds as first-order interpretations for Folds #2 and #3. We stress, however, that the causative faults for these two folds are not exposed in outcrop.

There are no rock properties built into these geometrical models, which may yield fold shapes that differ from real-world structures. There is, however, a geometric relationship between fault shape and fold shape. Hence, the term "fault-related folding" is often used, although it includes more than these two principal types of folding (see Shaw et al., 2005). Interpretations can be generated both graphically and analytically based on the theories. Detailed explanations of fault-bend and fault-propagation folding can be found in Suppe (1983), Suppe and Medwedeff (1990), and Shaw et al. (2005).

Although other modes of contractional, fault-related folding have been proposed, e.g., Erslev's (1991) tri-shear fault-propagation folds, they are more difficult to apply and generally involve changes in stratal thicknesses. This applies to Suppe and Medwedeff's (1990) fixed-axis, fault-propagation folds as well. Tri-shear interpretations must be applied iteratively and cannot be applied graphically or analytically (Shaw et al., 2005, p. 31). The features common to all these fault-propagation fold theories is that the fold forms at the fault tip and consumes slip (Shaw et al., 2005, p. 26). Common geometric characteristics include asymmetric folds with forelimbs steeper than back limbs; front synclinal axes pinned to the fault tip in early stages of development; and slip on the fault that decreases upward, often terminating within the fold (Shaw et al., 2005, p. 26).

Suppe and Medwedeff (1990, p. 439) emphasize that "… there are significant difficulties in comparing map-scale structures with theory." Map-scale structures are not completely exposed and often contain preexisting faults, folds, and unconformities, which may not be addressed specifically by these theories, especially in initial interpretations. Fold shape is often constrained in outcrop, but fault shape is usually poorly known or unknown. Decisions about the origin of map-scale folds are, therefore, made on incomplete data. The quantitative relationship between fold shape and fault shape in fault-related folds means that interpreted fault shape is predicted by theory and is not arbitrarily chosen.

Our interpretations assume perfectly angular fold hinges and fault bends. These angular approximations allow for rigorous area and line-length balancing and are built into the fault-related fold theories (Suppe, 1983, 1985; Suppe and Medwedeff, 1990). However, real-world folds generally exhibit some degree of curvature (Shaw et al., 2005). Medwedeff and Suppe (1997) explore multi-bend fault-bend folding as a way to impart curvature into the folding process. In this paper, we approximate the folds in the Quebradas region with perfectly linear limbs, angular fold hinges, and angular fault bends.

We begin with some background information of fault-bend and fault-propagation folding.

BACKGROUND

Fault-bend Folding

Basic concept

The basic need for fault-bend folding is illustrated in Figure 2, which shows a hypothetical cross section of a continuous, nonplanar fault that is composed of two planar segments with differing dips forming a concave-upward (synformal) fault bend (Shaw et al., 1994). Rigid-block translation (Fig. 2A) of the hanging-wall block (HW) over the footwall block (FW) along the fault produces two end-member solutions. If the HW stays in contact with the upper fault segment, a void is created between the HW and FW. If the HW stays in contact with the lower fault segment, the HW and FW overlap. Both cases are unreasonable: rocks are not strong enough to support large voids, and two bodies (of rock) cannot occupy the same space at the same time.

If, however, the HW folds through the development of a kink band, fault slip is accommodated without generating either a void or an overlap with the FW (Fig. 2B). Fault-bend folding is localized along an active (folding) axial surface that is fixed (pinned) to the bend in the fault in the FW. After folding at the active axial surface, strata are translated rigidly along the upper fault segment. The inactive (non-folding) axial surface is the locus of particles that were located along the active axial surface at the initiation of fault slip. The inactive axial surface is fixed in the HW and moves away from the active axial surface with progressive fault slip. Axial surfaces bisect inter-limb angles because stratal thickness is conserved. The width of the kink band, bounded by the axial surfaces, is proportional to the fault slip. Similarly, a kink band forms and widens over a concave-downward (antiformal) fault bend (not illustrated here, but explained in Shaw et al., 2005, p. 15).

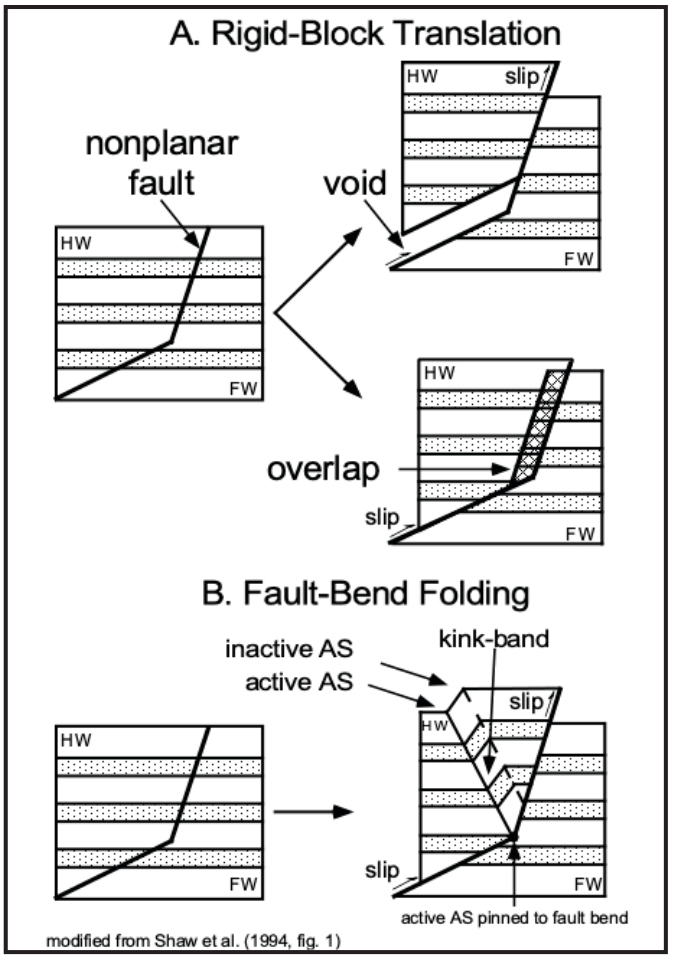

FIGURE 2. A fundamental concept of fault-related folding is that strata fold by kink-band migration as the hanging wall (HW) moves over a bend in a nonplanar fault in the footwall (FW). Rigid block translation of the HW past the bend would create either a void or an overlap with the footwall (**A**), neither of which is realistic at depth. Folding of the HW by development of a kink band accommodates fault slip without creating either a void or an overlap (**B**). Modified from Shaw et al. (1994, fig. 1).

Progressive development of a simple fault-bend fold

A common type of fault-bend fold involves deformation above a thrust ramp that connects lower and upper detachments, such as the Pitas Point anticline, Santa Barbara Channel, California, and the Tunic anticline, Sullivan County, Pennsylvania (Shaw et al., 1994, figs. 8 and 13, respectively). These folds are known as simple (or simple-step) fault-bend folds or flat-ramp-flat anticlines. In some cases, the upper detachment is the former land surface. Shaw et al. (2005, p. 21) refer to these folds as composite fault-bend folds.

Figure 3 shows geometrical models of this fold type as slip increases from zero (step 0) through maximum structural relief (step 2) and beyond (step 3). These models, which are modified from Suppe (1983, fig. 3) and Shaw et al. (2005, p. 21), allow a more detailed analysis of the theoretical folding process.

We follow Shaw et al. (1994, 2005) in the explanation of the development of a simple fault-bend fold. We quote Shaw et al.'s (2005, p. 21) description of the folding process and add our own comments (shown without quotation marks). Shaw et al. (2005) contains a CD-ROM with digital files of their diagrams. On Figure 3, we use Shaw et al.'s (2005, p. 21) lettering convention: "A" for back-limb axial surfaces and "B" for front-limb axial surfaces. (Suppe [1983, 1985] uses "B" for back-limb axial surfaces and "A" for front-limb axial surfaces.)

The progressive development of a simple fault-bend fold—also called the kinematic development by Suppe (1983, fig. 3)—is divided into two stages called the crestal uplift stage (Fig. 3, steps 1–2) and the crestal broadening stage (Fig. 3, step 3). During the crestal uplift stage, front and back limbs widen while structural relief of the fold increases with progressive slip. During the crestal broadening stage, the crest widens with progressive slip, but the limb widths and structural relief of the fold are fixed. (Note that we follow Suppe [1983, 1985] and Shaw et al. [2005] in using the term "width" to describe what others may call the "length" of a fold limb. The width parameter can be measured directly on the limb between the paired axial surfaces that bound the limb.)

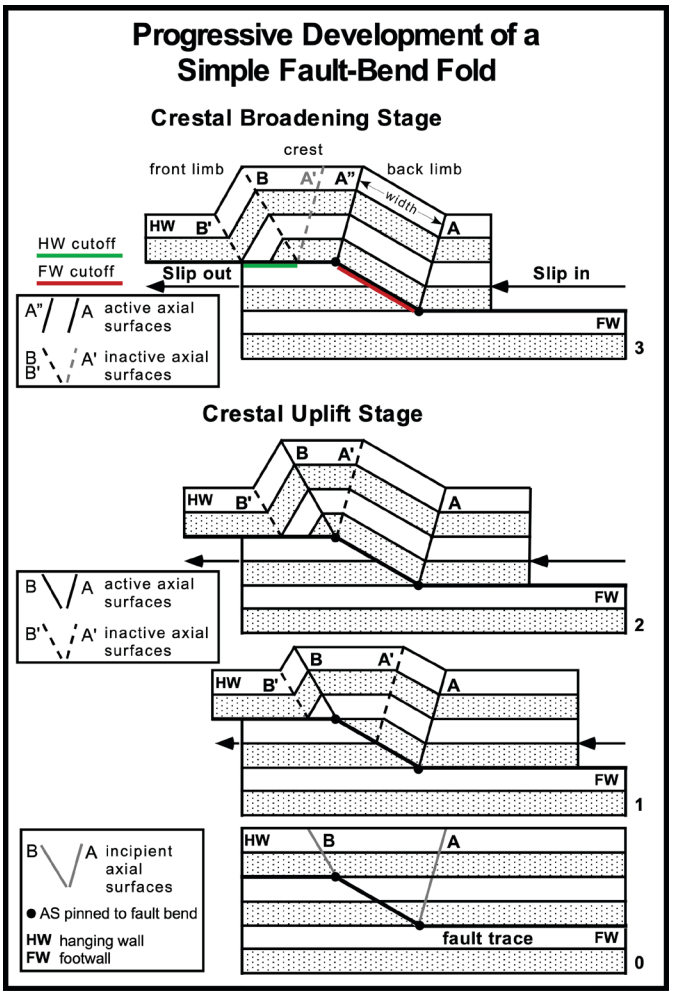

FIGURE 3. Progressive development of a simple fault-bend fold in two stages. During the crestal uplift stage, fold limbs widen and structural relief increases as fault slip increases (steps 0–2). During the crestal broadening stage (where fault slip exceeds ramp length), limb widths and structural relief are fixed and the crest widens (step 3). Modified from Suppe (1983, fig. 3) and Shaw et al. (2005, p. 21).

Step 1: Initiation of slip causes the hanging wall block (HW) to fold along active axial surfaces A and B, which are pinned in the footwall (FW) to the two fault bends. Inactive axial surfaces A' and B' form in the HW above the fault bends; they are initially coincident with active axial surfaces A and B, but are passively translated away from them by increasing slip (Fig. 3, steps 1–2). Progressive fault slip widens both the front- (B-B') and back- (A-A') limb kink bands as the crest of the fold is elevated. "Kink-band width A-A' or B-B' measured along bedding equals slip on the underlying fault segment. The difference in kink-band width between back and front limbs reflects slip consumed in folding."

Step 2: Progressive fault slip widens both kink bands and increases structural relief. (Steps "1 and 2 are in the crestal uplift stage because the fold elevates with increasing fault slip.")

Step 3: After axial surface A' reaches the upper fault bend, increasing fault slip causes "…material from the back limb to be refolded onto the crest and the front-limb kink-band is translated along the upper detachment." In the crestal broadening stage, "…A and A" are active axial surfaces; B and B' are inactive axial surfaces."

Step 3 "… is in the crestal broadening stage because the fold crest widens without producing additional structural relief with increasing fault slip. In the crestal broadening stage, slip exceeds the width of the back limb and is equal to the distance between axial surfaces A and A' measured along the fault." Inactive axial surface A' separates rocks on the crest that have the same dip but different structural histories. Rocks to its left are horizontal but have never been folded; rocks to its right are horizontal but have been folded twice.

Front-limb dip and the slip ratio (R = slip-out/slip-in) for a simple fault-bend fold is a function of the initial step-up angle of the ramp relative to bedding; back-limb dip in the simplified example shown in Figure 3 is equal to the step-up angle (from Suppe, 1983). In general for fault-bend folds, the step-up angle of the fault relative to bedding is not equal to the change in dip of the fault segments.

TABLE 1. Dips and slip ratios for simple fault-bend folds at selected step-up angles, modified from Suppe (1983). (R = slip-out/slip-in).

Step-up angle	Back-limb dip	Front-limb dip	Slip ratio (R)
5°	5°	5°	0.99
10°	10°	10°	0.97
15°	15°	16°	0.93
20°	20°	23°	0.87
25°	25°	33°	0.78
26°	26°	35°	0.76
27°	27°	38°	0.73
28°	28°	42°	0.70
29°	29°	47°	0.66
30°*	30°	60°	0.58

*Maximum step-up angle for simple fault-bend folds without relaxing the constant-thickness requirement.

Geometric patterns apparent in these models allow for geologic predictions that could improve interpretations, whether in outcrop or on seismic-reflection profiles. Depth to detachment is important in making complete cross sections from shallowly imaged structures or partially exposed structures. A complete cross section is one that extends deep enough to reveal the fundamental nature and origin of the structure (Suppe, 1985).

A maximum depth to the upper detachment of any simple fault-bend fold can be estimated by projecting the two (non-parallel) axial surfaces that bound its crest (A' and B in steps 1 and 2, and B and A" in step 3 of Fig. 3) downward until they converge. If the fault-bend fold is at the top of the crestal uplift stage (Fig. 3, step 2), the axial surfaces converge exactly at the upper detachment. At all other stages of development (Fig. 3), the convergence point is below the upper detachment. A maximum depth to the lower detachment can be obtained by extrapolating the fault ramp downward from this convergence point until it intersects the back synclinal axial surface (A). In this simple case, the back limb and ramp have the same dip because the fault steps up from a bedding-parallel detachment. In many outcrop examples, the fault steps up from a lower ramp segment, not a detachment. Movement on this fault segment places the undeformed (horizontal) strata in the hanging wall that were initially behind the structure at a higher structural elevation than the equivalent undeformed footwall strata in front of the fold. In fold segments and partially imaged or exposed folds, hanging-wall and footwall cutoffs are identified by patterns of dipping beds above the fault segment and horizontal beds below (see Fig. 3, step 3). The hanging-wall cutoff is formed by the more steeply dipping beds of front-limb kink-band B-B' that are separated by the upper detachment from horizontal beds in the footwall. The footwall cutoff is formed by horizontal beds in the FW that are separated by the ramp fault from the dipping beds of the back-limb kink-band A-A'.

Fault-propagation Folds

Some folds appear to have developed in front of propagating faults (Suppe, 1985). In the absence of a throughgoing fracture, all the slip on the fault must be consumed in the folding process. Suppe (1985, p. 350) notes that some major thrust faults in the Canadian Rockies die out in the cores of folds. In outcrop, these thrust faults commonly terminate at the front synclinal axial surface of the fold.

Suppe (1985) defined and Suppe and Medwedeff (1990) refined fault-propagation folding theory, which is also a two-dimensional, geometrical, and kinematic theory with the same built-in balancing assumptions of conservation of bed thickness, line length, and area that are found in fault-bend folding. However, the fold forms at the fault tip as the tip propagates. There is a quantitative relationship between fold shape and fault shape.

Fault-propagation folds typically have narrower, steep-to-overturned front limbs, longer back limbs, and greater structural relief than comparable fault-bend folds that step up at the same angle. The fold forms above the ramp by kink-band migration in which axial surfaces bisect the angles between

adjacent kink bands. Fault-propagation folds that step up from a bedding plane detachment are known as simple-step fault-propagation folds. They are more complex than simple fault-bend folds and have five axial surfaces, three of which are active (Fig. 4). One big difference is that an active, synclinal axial surface (A') is pinned to the fault tip. As strata pass through A', they are folded into the front limb. The discussion of the sequential development of a simple-step fault-propagation fold that follows is based on Figure 4, but is considerably less involved than that in Suppe and Medwedeff (1990), which includes a complete quantitative analysis of the theory. (Note that we use Suppe and Medwedeff's [1990] lettering convention for the axial surfaces of a fault-propagation fold because Shaw et al. [2005, p. 27] do not label the axial surfaces.)

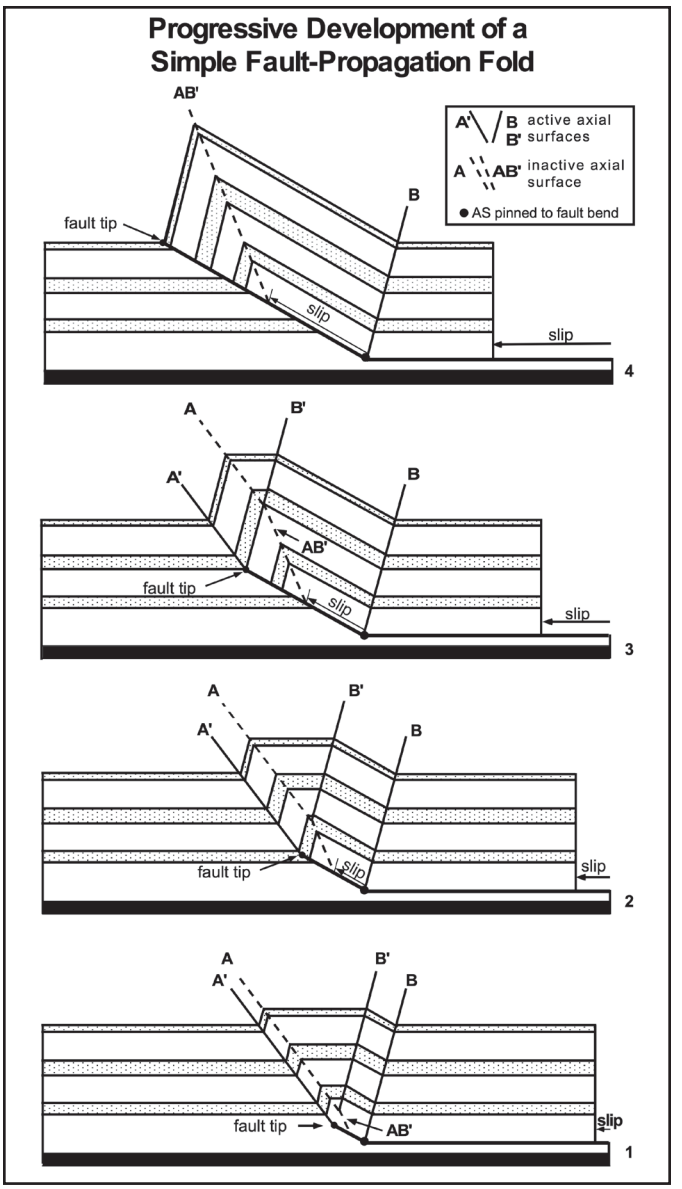

FIGURE 4. Progressive development of a simple fault-propagation fold. As slip increases, the front and back limbs widen, the flat crest narrows, and structural relief increases (steps 1–3). When the fault tip reaches the surface of the earth (step 4), the flat crest has been consumed and structural relief and limb widths are fixed. Modified from Suppe and Medwedeff (1990, fig. 6).

Progressive development of a simple fault-propagation fold

At the initiation of slip, as the fault steps up from the bedding-plane detachment (Fig. 4, step 1), two kink bands form, one between axial surfaces A and A' and the other between axial surfaces B and B' (referred to as kink bands A-A' and B-B'). Active axial surface B is pinned to the synformal bend in the fault (at the base of the footwall ramp) and beds pass through it onto the back limb of the fold. As active axial surface B' moves through the fold as the slip increases, beds pass through it from the crest to the back limb, increasing the width of the back limb and reducing the width of the crest. Active axial surface A' is pinned to the fault tip, forming the front synclinal surface, and beds roll through it onto the front limb (from left to right in Fig. 4) as the fault propagates. Inactive axial surface A moves away from A', widening the front limb. Axial surface AB' forms by the merging of axial surfaces A and B' as the horizontal crest is annihilated; this axial surface is the only axial surface fixed in the material. When the fault tip reaches the top of the uppermost bed, often the surface of the earth, the crest has been completely consumed (Fig. 4, step 4).

Front-limb dip of a simple-step fault-propagation fold is a function of the initial step-up angle of the ramp relative to bedding; back-limb dip is equal to the step-up angle, as illustrated in Table 2.

TABLE 2. Front- and back-limb dips for a simple-step fault-propagation fold, stepping up at various angles, modified from Suppe (1985).

Step-up angle	Back-limb dip	Front-limb dip
10°	10°	141°
15°	15°	122°
20°	20°	105°
25°	25°	88°
30°	30°	72°
35°	35°	58°
40°	40°	45°

Note: Dips greater than 90° are overturned.

Some geometric patterns apparent in these models during early stages of development (Fig. 4, steps 1–3) that allow for geologic predictions that could improve interpretations include: (1) the back-limb width, measured along any bed in kink band B-B', is twice the slip; (2) the fault tip is in the same bed in which axial surfaces A and B' intersect; (3) the front synclinal axial surface A' intersects the fold at the fault tip; and (4) axial surface AB' intersects the fault ramp at the point equal to the fault slip, which is exactly halfway up the ramp between the fault bend and the fault tip, but only in the simple-step fault-propagation fold, so that slip is equal to one-half of the ramp width.

As fault-propagation folds continue to absorb fault slip, the fold can lock up. New faults, called breakthrough faults, frequently occur at zones of weakness in the fold. These new faults alter the geometry of the original fold. Suppe and Medwedeff

(1990, fig. 11) delineate five types of breakthrough structures, each with a unique geometry. A fault-propagation fold with high-angle breakthrough is described later in this paper.

FAULT-RELATED FOLDS ALONG THE QUEBRADAS BACK COUNTRY BYWAY

Pattern Recognition Using Generic Fault-related Folds

In compressional environments such as fold and thrust belts, fault systems transfer slip from deep, commonly bed-parallel detachments (or decollements) to the surface of the earth via one or more ramps that cut across strata. The ramp and run geometries that generate fault-bend folds form when faults exploit weak bedding planes and existing low-angle fractures. When faults encounter areas with neither weak detachment surfaces nor properly oriented fractures, fault-propagation folds can form. These two types of folding produce different patterns (Figs. 3 and 4) that will be used to initiate interpretations of the folds in the Quebradas region.

Figure 5 summarizes some of the differences between the simple fault-bend and fault-propagation folds that were shown in Figures 3 and 4. This diagram presents a generalization of each fold's characteristics at an early stage of growth. Simple fault-bend folding produces a roughly symmetrical fold above a nonplanar, throughgoing (continuous) fault that steps up abruptly at a low angle (fault ramp) from a lower detachment (lower flat) to an upper detachment (upper flat). More slip enters than exits the fold, a requirement of conservation of line length and bed thickness that leads to the front limb being steeper than the back limb.

Simple-step fault-propagation folding produces an asymmetrical fold that forms at the tip of a propagating fault that steps up abruptly from a detachment; the front limb is shorter and usually much steeper than the back limb. The fault dies out in the core of the fold and the front synclinal axis emanates from the fault tip. All the slip that enters the fold is consumed in fold-related shortening. Both fold types in Figure 5 are generated above faults that step up at low angles (<25°) relative to bedding.

In the initial phase of an interpretation, our emphasis is on recognizing patterns and making first-order inferences based on those patterns that would likely be refined with further investigation; it is not in matching the exact geometry of the outcrop with the model. To that end, we use these "off-the-shelf," generic fold models (Fig. 5) to recognize patterns in an outcrop in the southern part of the Quebradas region (Fig. 1).

Fold #1: Complex structural deformation in Permian rocks

An illustrative complex of folds and faults is well exposed in profile view on the ~6 m high, south wall of an unnamed arroyo, located ~30 m east of the Quebradas Byway (Fig. 1, Fold #1; 33.983488°N, -106.761694°W, WGS84; SE1/4 SE1/4 SW1/4 sec. 5, T. 4 S., R. 2 E., San Antonio 7.5-minute quadrangle). We postulate that the structural styles seen here may, in microcosm, represent those seen across the Quebradas region. Patterns representative of both fault-bend and fault-propagation folds are highlighted in the red and yellow sandstones in the Meseta Blanca Formation (Arroyo de Alamillo Formation *sensu* Lucas et al., 2005) and the overlying gray limestone in the Torres Member of Los Vallos Formation (Fig. 6). Our discussion is limited to the structural features we consider important to the interpretation of folds throughout the Quebradas region. This discussion is not all inclusive; in some cases, only portions of faults and folds are highlighted and discussed.

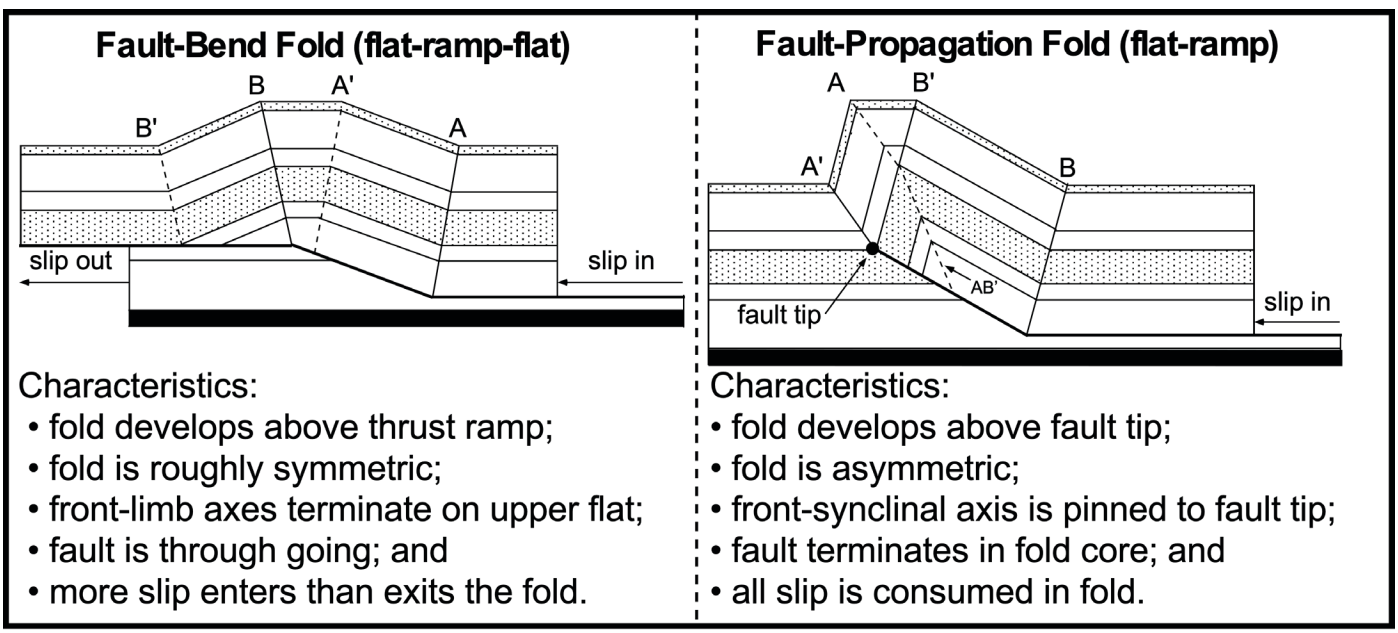

FIGURE 5. Comparison of general geometric characteristics of a simple fault-bend fold (A) and a simple fault-propagation fold (B), based on comparable growth stages shown on Figures 3 and 4.

This outcrop (Fig. 1, Fold #1) was also discussed by Smith et al. (1983, p. 19–20) and Scholle (2010, Stop 8). It is included as Stop 2 on Day 1 of the 2022 New Mexico Geological Society Fall Field Trip (Koning et al., this volume).

To generate our first-order interpretations, we assume perfectly angular fold hinges and fault bends. The linear dip domains annotated on the photograph are approximations that allow us to locate positions of axial surfaces. The beds may have some curvature but have been "averaged out" by straight lines.

Feature 1: The most apparent structure in this outcrop is a small, asymmetric anticline at the east (left) end of the photograph just above the base of the arroyo (Fig. 6). This fold has developed above a nonplanar thrust fault that steps up to the east from a detachment and dies out in the core of the fold. A flattish crest separates a shallowly dipping limb on the west from a more steeply dipping limb (composed of two kink bands) on the east. The core of this fold can be modeled quite well with the linear kink-band segments; there is little deviation from linearity in the beds labelled #1 and #2. Dip domains in the middle part of the fold (primarily in the yellow sandstone) are not as linear and differ from those in the lower part of the fold, reflecting additional folding on other thrust faults higher in the section (not annotated in Fig. 6); these faults step up to the east and duplicate strata above the small fold's crest. The uppermost part of the fold is cut by a horizontal thrust fault, above which the basal limestone of the overlying Torres Member of Los Vallos Formation is duplicated (above the abandoned nest).

The core of this fold is delineated by two thin (<20 cm thick), white sandstone beds (labeled #1 and #2) in the lower red unit of the Meseta Blanca, whereas the upper part of the fold is delineated by the contrast between the red and yellow units in the Meseta Blanca and the gray limestone at the base of the Torres Member. The causative fault enters the fold from

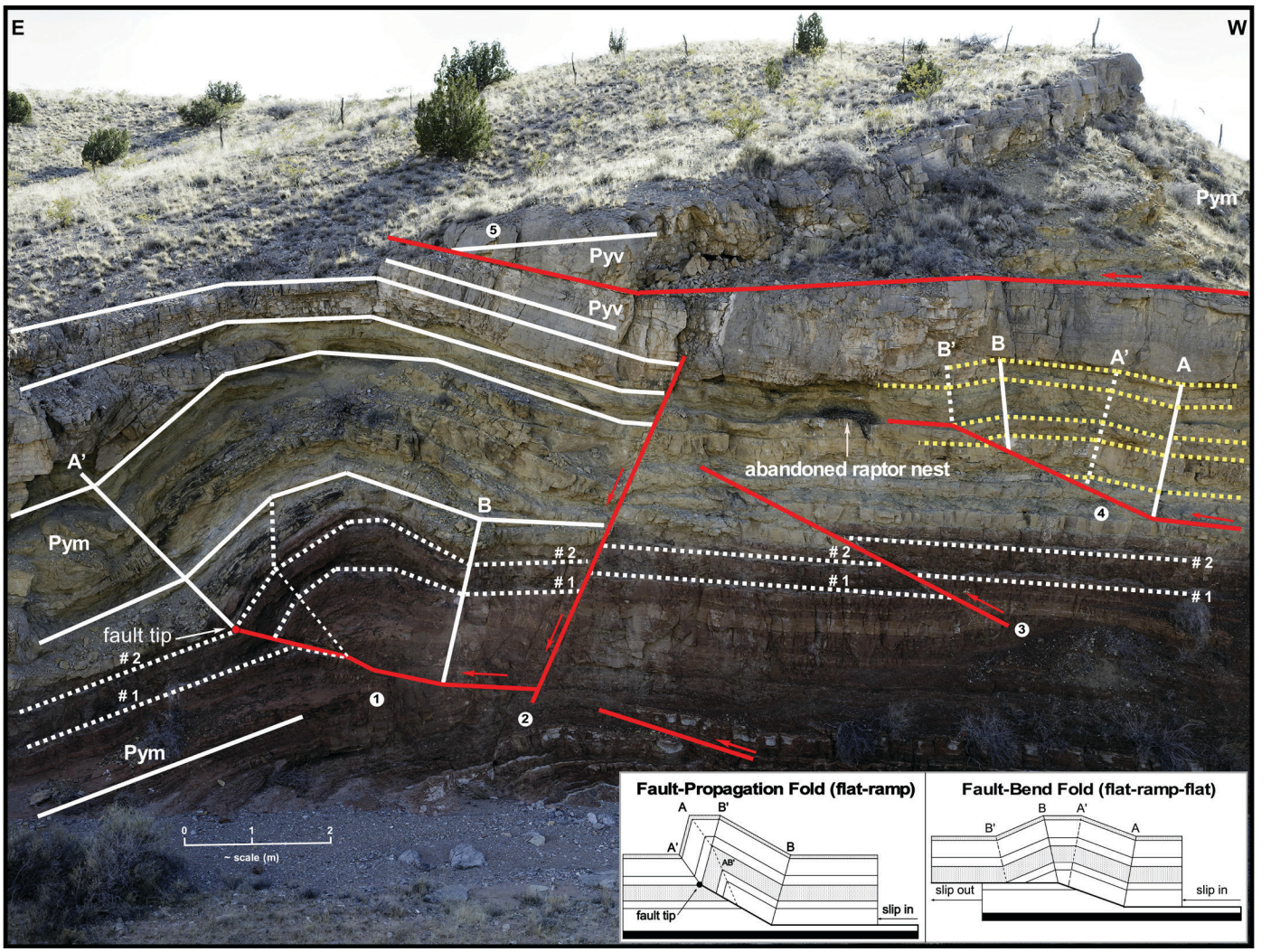

FIGURE 6. Fold #1. Image of the south wall of an unnamed arroyo 5.4 km south of Arroyo de las Cañas (Fig. 1, Fold #1; 33.983488°W, -106.761694°N, WGS84). Not all strain features are annotated. This profile-view exposure highlights the structural complexity of the Quebradas region and illustrates both fault-bend and fault-propagation folds that developed above non-planar fault segments. Slip on segments of planar normal and reverse faults has translated beds up or down the fault without dip change or drag. Pyv = the Torres Member of Los Vallos Formation of the Permian Yeso Group; Pym = the Meseta Blanca Formation of the Yeso Group. Faults are red; axial surfaces are labeled as A, A', B, and B'; bed attitudes for the eastern fold are highlighted in white short dashes; and bed attitudes for the western fold are shown in yellow short dashes. Other stratal contacts are shown as white continuous lines. Structural features discussed in the text are labeled inside white circles. Inset provides direct comparison with general models. (Photograph courtesy of Don Boyd Photography.)

the west along a bedding plane, runs along the top of bed #1 (which is subparallel to the fault), and terminates against bed #2. The lower white bed (#1) is folded but continuous in the hanging wall above the fault. The upper white bed (#2) is folded continuously both above and below the level of the fault. Bed #1 is offset along the ramp by ~1 m; bed #2 is not offset and the fault terminates against it. The front synclinal axial surface of the fold (A') emanates from this fault termination. Both numbered beds are parallel below the level of the ramp fault, where they dip 22°E and form the eastern limb of a lower fold.

In the fold's core, the two numbered beds are folded into four, well-defined, angular kink bands. The fold's flattish crest is bounded by a shallowly dipping back limb on the west and a more steeply dipping front limb on the east that is composed of two kink bands that steepen downward. Both the back and front synclinal axes are well delineated by the numbered beds. The front synclinal axis (A') of the fold terminates at the fault tip. The back synclinal axis (B) projects into the fault ramp at the initial synformal bend linking the ramp to the detachment. This ramp has at least two other dip changes upward along its trace, including another synformal bend followed by an antiformal bend. The additional bends contribute complexity to the fold's geometry.

This small fold has sufficient features in common with the simple fault-propagation fold model (Fig. 6, inset) that it can be interpreted as a fault-propagation fold. The common features include: a thrust fault that ramps up from a bedding plane detachment; an asymmetric anticline developed above and in front of the fault ramp; a steeper front limb than back limb; fault slip that dies out into the fold's core; bed offset that decreases upward to zero along the fault; a front synclinal axial surface that terminates downward at the fault tip; and a back synclinal axis that terminates at a synformal bend in the ramp fault. This small fold differs from the simple model in having more bends in the fault ramp (at least three), more dip panels (kink bands) in the fold, and non-horizontal beds in front of and below the ramp likely related to some other strain feature. In the model, the bed at the fault tip has only two segments of unique dips corresponding to the back limb and front limb. In the outcrop, a small flat crest is present in both bed #1 and bed #2, the result of kink bands associated with multiple bends in the fault ramp.

In a multi-bend fault-propagation fold, each bend in the fault generates a kink band, bounded by an active and an inactive axial surface. With progressive slip, these kink bands grow, merge, and interfere with each other, and create new axial surfaces and dip panels (Shaw et al., 2005, p. 22). These predicted dip panels cannot be entirely differentiated at the scale of this fold and the resolution of the photograph. Approximating the closely spaced, multiple fault-bends in the ramp by a single bend that steps up at ~30° (to match the back-limb dip of bed #2), predicts a steep, but not overturned, front-limb dip of 72° (Table 2). This predicted dip is similar to the actual forelimb's steeper dip of 62° and is similar to the generic fault-propagation fold (inset). White sandstone bed #1 has been offset ~1 m to the east from the west end of where the bed is subparallel to the fault in the footwall. Total slip on the fault is estimated to be ~2.6 m based on half the width of the ramp (as noted earlier, in a simple-step fault-propagation fold, the slip is equal to half of the width of the fault ramp). The unique feature of this fault-propagation fold in the Quebradas region is that the causative fault is exposed in the outcrop.

Features 2 and 3: West (right) of synclinal axial surface B, horizontal beds #1 and #2 are offset by a planar, high-angle normal fault that dips ~62°E (feature 2). Farther west, these same beds are offset by a planar, low-angle reverse fault that dips ~28°W (feature 3). In both cases, the numbered beds have been translated rigidly with no change in dip. These two faults are only partially interpreted on the photograph to emphasize that strata displaced along planar fault segments have not folded (i.e., changed dip).

Feature 4: At the west (right) edge of the image, a small fold (bed attitudes shown in yellow) is present above a thrust fault that steps up to the east at ~25° between two detachments near the top of the Meseta Blanca Formation. This fold is similar to the generic fault-bend fold (inset) in several respects. The fold is developed above the ramp; the front and back limbs dip at shallow angles and are separated by a flattish crest; and the back limb is wider than the front limb. The back limb is ~1.0 m wide and the front limb is ~0.8 m wide. These limb widths yield an "R" value of ~0.8, almost exactly the predicted value for a 25° step-up angle (Table 1). The front-limb dips ~10°E, considerably less than the predicted 33°. The back limb dips ~10°W, also considerably less than the predicted 25°. The biggest difference between this fold and the model is that the front limb formed above the ramp, not the upper detachment. The east-dipping beds of the hanging-wall cutoff in the front limb of this fold are now above the same beds that are horizontal in the footwall below the fault.

Feature 5: At the top of arroyo wall, in the middle of the image, the lower part of the Torres Member and the upper part of the Meseta Blanca Formation are duplicated above a horizontal thrust fault that has at least 10 m of easterly directed slip on the upper detachment of a fault-bend fold. The hanging-wall cutoff of the Torres Member is juxtaposed on Torres Member in the footwall, producing a pattern similar to that in the small fault-bend fold (in yellow) to the west.

Interpreting this outcrop as a microcosm of the structural features present in the Quebradas region indicates that fault-related folding with easterly directed slip is an operative contractional folding mechanism. All the reverse-fault segments are either bedding-plane parallel or step up to the east at low angles (<25°) relative to bedding. The only steep fault (>45°) in the outcrop is a younger, normal fault that dips ~62°E. These data indicate that some Quebradas folds formed above detachments or shallowly dipping ramps and are not associated with steep faults that originate in the basement. Based on this assessment, we will use the simple fault-bend and simple fault-propagation fold models to approximate two other folds in the Quebradas region (Folds #2 and #3 below).

This outcrop provides a natural example of the main tenet of fault-related folding: folds form only above nonplanar faults. If the faults are planar, the beds are translated rigidly either up or down the fault. If the fault is nonplanar, the beds change dip as they move past the bend in the fault and they deform by kink-band migration.

At the next stop, Fold #2, with this outcrop in mind, we interpret a large anticline with an overturned front limb as a fault-propagation fold.

Fold #2: Fault-propagation fold in Arroyo del Tajo

At a distance of 0.5 km west of the Quebradas Byway, incision of Arroyo del Tajo has exposed a large fold in the Pennsylvanian Atrasado Formation (Fig. 1, Fold #2; 34.048735°N, -106.781256°W, WGS84; SW1/4 NW1/4 sec. 18, T. 3 S., R. 2 E., Loma de las Cañas 7.5-minute quadrangle). The oblique cross section exposed on the north canyon wall (Fig. 7) consists of an asymmetric fold that has a long, moderately dipping limb on the west, an angular crest, and an overturned limb on the east (Fig. 7). As shown in the photograph, the west limb is ~35 m wide and dips ~22°W; the east limb dips ~ 60°W—bent ~120° from its originally horizontal position. The fold is ~40 m wide in the canyon (measured using the innermost, resistant limestone bed at arroyo level). Approximately 30 m of structural relief, corresponding approximately to the amplitude of the fold, is visible above the arroyo floor. The causative fault is not exposed in the arroyo. Resistant beds seem to be symmetrically arranged on either side of the interior anticlinal axial surface, although they are upside down on the east (right) limb. This outcrop was discussed by Smith et al. (1983, p. 18) and is also included as part of Stop 3 on Day 1 of the 2022 New Mexico Geological Society Fall Field Trip (Koning et al., this volume). These folds are part of the Laramide Tajo structural zone, an arcuate array of reverse faults and associated folds striking ~030° (Cather and Axen, in press).

Comparison of this fold to the general fold types (Fig. 5) suggests that this natural cross section can be interpreted as a simple fault-propagation fold that stepped up toward the east and has an overturned front limb (Fig. 7, inset). Comparison of the dips measured on this oblique cross section to a theoretical model indicates that there is a close approximation between the two. A theoretical, simple fault-propagation fold stepping up at the measured, back-limb angle of ~20° would have an overturned front-limb dip of 105° (Table 2). Step-up angles of 20° to 15° would produce front-limb dips of 105° to 122°.

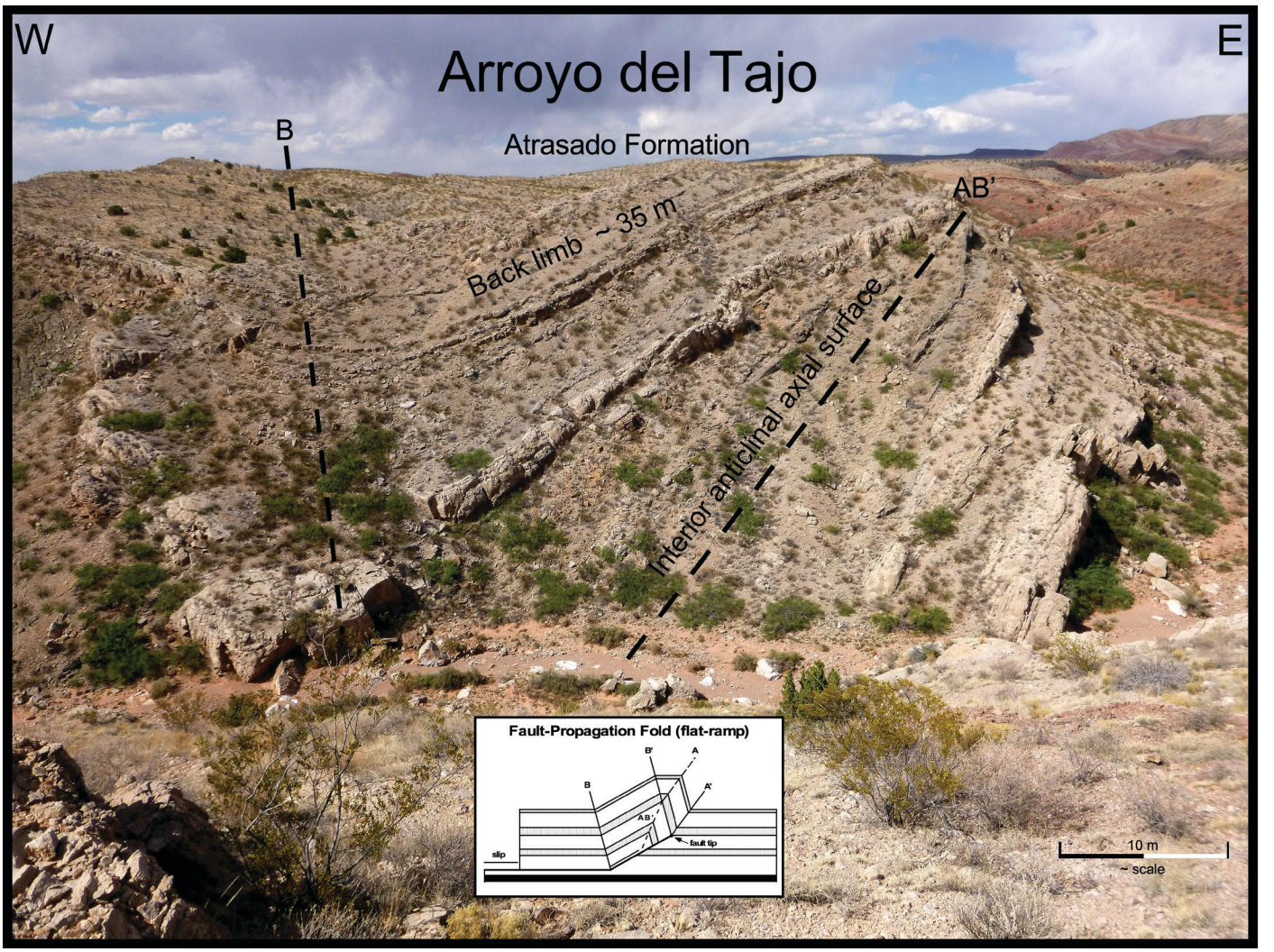

FIGURE 7. Fold #2. Image of the north canyon wall of Arroyo del Tajo (34.048735°W, -106.781256°N, WGS84), showing an asymmetric fold with an overturned front limb that developed in the Pennsylvanian Atrasado Formation (Fig. 1, Fold # 2). Inset for comparison with general model. The location of Fold #2 is shown on Figure 8. (Photograph courtesy of David Love.)

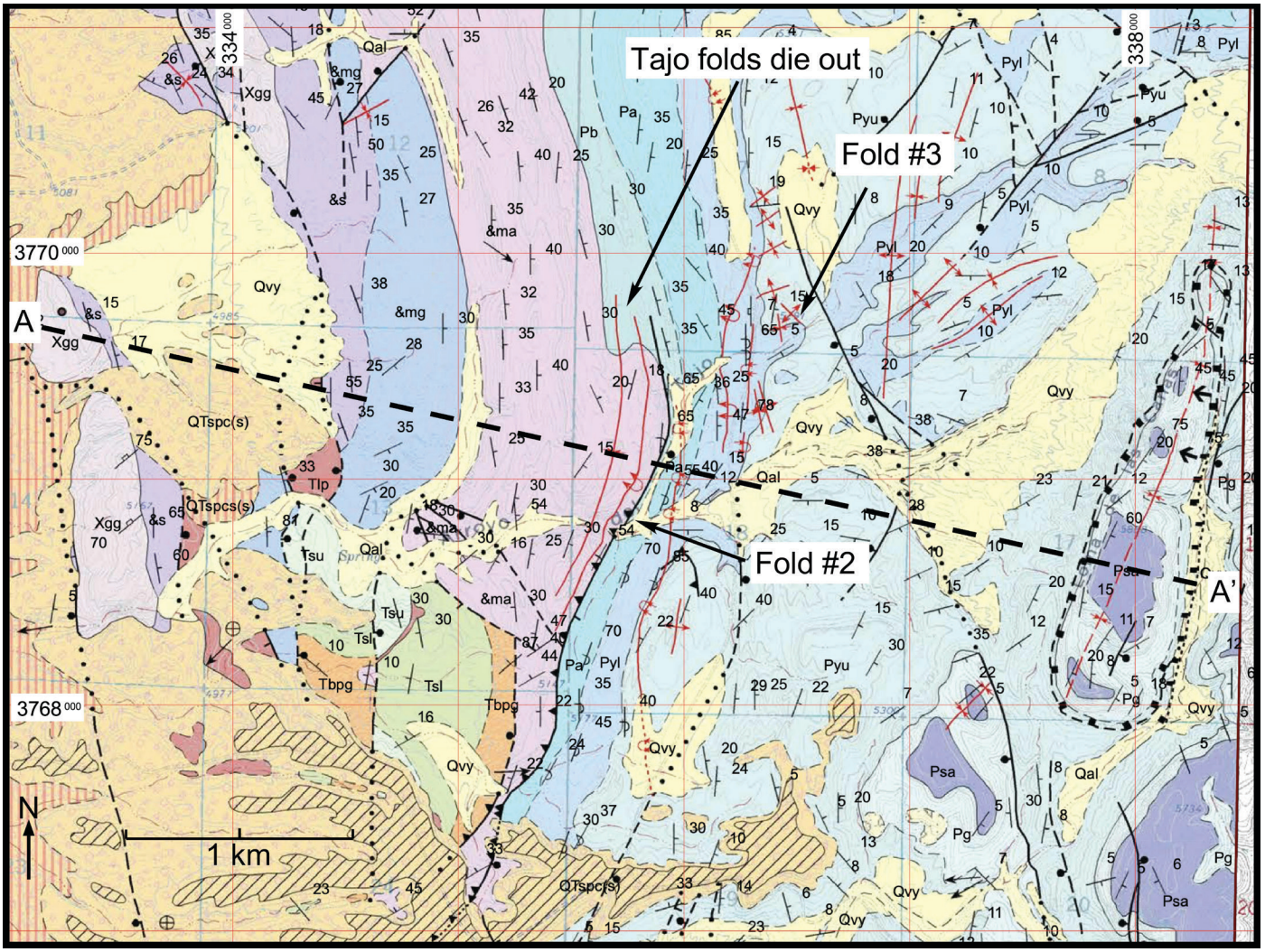

FIGURE 8. Portion of the Loma de las Cañas geologic quadrangle map (Cather and Colpitts, 2005) centered on Arroyo del Tajo showing the locations of cross section A-A' and Folds #2 and #3. Abbreviations of important map units (ascending): Xgg—Precambrian granite; &s—Pennsylvanian Sandia Formation; &mg—Penn. Gray Mesa Formation (Madera Group); &ma—Penn. Atrasado Formation (Madera Group); Pb—Permian Bursum Formation; Pa—Perm. Abo Formation; and Py—Perm. Yeso Formation. (Note that "&" is the symbol used on the map for Pennsylvanian units.)

Fault-propagation folds are frequently complicated when the causative fault locks up and breaks through the fold from some point along the original fault ramp on a new trajectory (Suppe and Medwedeff, 1990). As a breakthrough fault cuts across the fold, it alters the fold's geometry. A breakthrough can occur when the fold can no longer grow self-similarly because of rock properties that change in front of the propagating fault. Suppe and Medwedeff (1990, p. 418) note that in such cases "…the fault breaks through the structure in a fracture mode…and often utilizes zones of weakness created along the anticlinal and synclinal axial surfaces in the front limb of the fold."

When the fault breaks through in "fracture mode," a throughgoing fault is created. Slip on this new fault creates a hybrid fault-propagation/fault-bend fold. Suppe and Medwedeff (1990, p. 419–422) discuss and illustrate five types of breakthroughs that can alter a simple fault-propagation fold, including decollement, synclinal, anticlinal, high-angle, and low-angle breakthrough.

In the fold at Arroyo del Tajo, Cather and Colpitts (2005) mapped a single thrust fault that cuts the font limb of the fold (Fig. 8). In addition, there is a mismatch of beds across the axial crest (Fig. 7). Both the fault and the mismatch near the interior anticlinal axial surface AB' are indications that breakthrough has occurred. Shaw et al. (2005) note that in some cases where slip on the breakthrough fault is substantial or the structure is deeply eroded, only remnants of the original fold remain. Fault-propagation fold breakthrough with deep erosion is probably the origin of an isolated, but large fragment of an overturned syncline developed in Permian strata at the southern end of the Tajo fold belt, approximately 3.0 km south of Arroyo del Tajo (Cather and Colpitts, 2005, fig. 1).

We illustrate and describe high-angle breakthrough as a first-order interpretation of the fold north of Arroyo del Tajo because it is the easiest of the breakthrough models of Suppe and Medwedeff (1990, fig. 11) to understand and it illustrates the breakthrough process. In high angle breakthrough (Fig. 9), the fault breaks through somewhere within the steep front limb

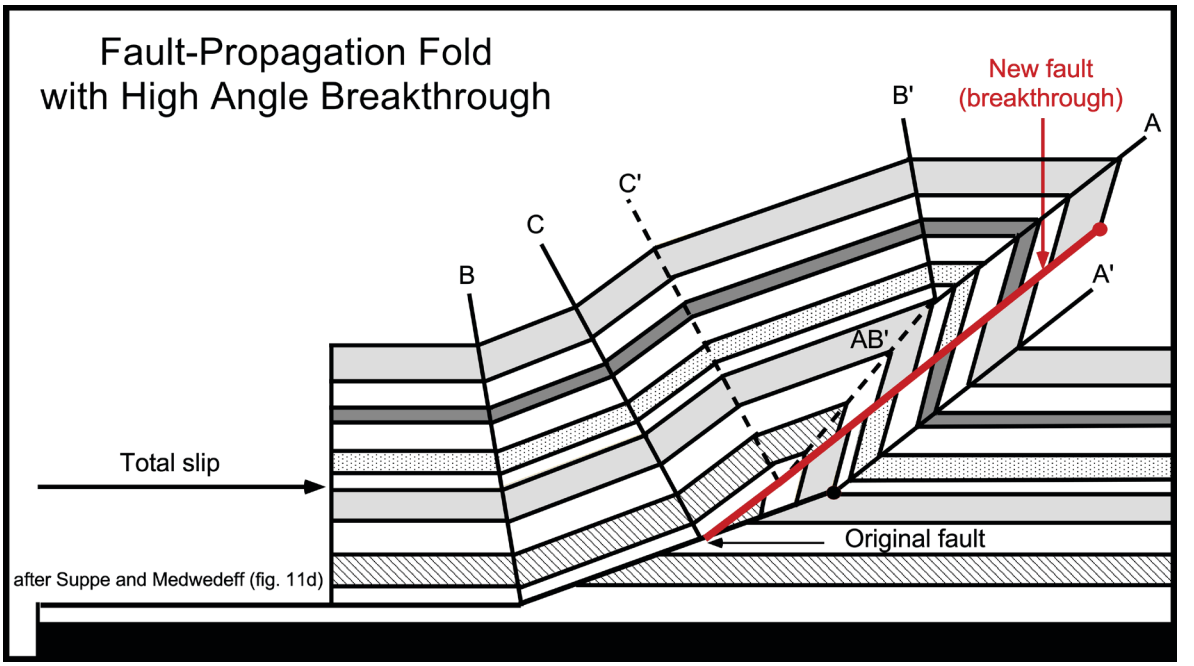

FIGURE 9. Model of a fault-propagation fold with high-angle breakthrough fault (modified from Suppe and Medwedeff, 1990, fig. 11d).

because of extensive preexisting fractures and, depending on the amount of subsequent erosion, can produce a "snakehead" anticline or an overturned syncline with the axial surface approximately parallel to the newly formed thrust fault (Suppe and Medwedeff, 1990, p. 419–422). One additional kink band (C-C')—formed at the new synformal bend in the fault—is created on the back limb.

Cather and Colpitts (2005) note that "…systems of tight fault-propagation folds…" occur in three areas on the Loma de las Cañas quadrangle. Their cross section A-A' (Cather and Colpitts, 2005) includes the fold north of Arroyo del Tajo (Fig. 8). Their interpretation involves a planar thrust fault that dips 40°W and comes directly out of the basement. Three sets of folds with overturned front limbs in the Pennsylvanian Sandia Formation, Gray Mesa Limestone, and Atrasado Formation are developed—one above the other—along this single fault. Cather and Axen (in press) also refer to these folds as fault-propagation folds. The interpretation of Cather and Colpitts (2005, cross section A-A') can be characterized as a "thick-skinned" interpretation of the Quebradas region, because the causative fault extends upward from the basement and involves the entire Paleozoic section in the folding process. However, none of their three folds is depicted as having formed in front of a propagating fault.

Our first-order interpretation relies on our understanding of fault-related folding as primarily low-angle faulting in which the folds are confined to a single thrust sheet and do not generally extend to depth. A fault-propagation fold is often confined at the surface to one or a few rock units, because the slip on the fault is consumed in the folding process and the step-up angle of the fault is low. Ultimately, however, the Precambrian and Paleozoic rocks had to be brought to the surface on higher-angle faults to the west of the Quebradas region. Lacking subsurface data, we postulate a model of a single fold formed above a low-angle thrust fault, similar to that illustrated in Figure 9.

Our "thin-skinned" interpretation offers three advantages over the "thick-skinned" interpretation of the Tajo folds. First, it is based on field observations of a well-exposed fold in the Quebradas region that formed above a thrust fault that stepped up at a low angle from a horizontal detachment (Fig. 6). Other folds at this outcrop also formed above nonplanar thrust faults. Second, this fold formed at the tip of a propagating fault and consumed all the slip on the fault. Third, fold shape and fault shape on the model are not arbitrary, but are the result of the application of rigorous geometric theory constrained by outcrop parameters. However, we emphasize that this is an interpretation and not a final solution. A strategically placed deep well or gravity survey could be used to test the competing structural models.

Fold #3: the "Yeso syncline"

The "Yeso syncline" is an outcrop-scale fragment of a breached fold (anticline/syncline pair) developed in Permian strata near the Los Vallos/Meseta Blanca Formation contact just to the east of the Byway (Fig. 10). It is part of the Tajo structural zone (Cather and Axen, in press) and is located about 0.6 km east of the forelimb syncline of Fold #2. The fold is named for its most prominent feature: an eroded, angular syncline developed in the Yeso Group. This informal name was first applied by Prof. Clay T. Smith (1917–2003), legendary geology professor at New Mexico Tech (pers. commun., 2002). The back syncline of the fold forms a conical hill that is capped by the resistant carbonate strata at the base of the Torres Member of Los Vallos Formation of the Yeso Group (Pyv). This conical hill (with a spot elevation of 5241 ft) is in the SW1/4 SE1/4 sec. 7, T. 3 S., R. 2 E., Loma de las Cañas 7.5-minute quadrangle (34.05368°N, -106.773860°W, WGS84). This outcrop

(Fig. 1, Fold #3) was also discussed by Smith et al. (1983, p. 18) and is included with Stop 3 on Day 1 of the 2022 New Mexico Geological Society Fall Field Trip (Koning et al., this volume).

Because strata are horizontal for 40 m to the west of the syncline axis (B in Fig. 10), we interpret that Fold #3 formed in relatively undeformed strata in front (east) of the overturned front limb of Fold #2 and east of synclinal axial surface A' (Fig. 9). The west portion of the angular syncline, which is highlighted by thin, red sandstone beds in the upper Meseta Blanca Formation of the Yeso Group (Pym), appears to be nearly horizontal in this view (Fig. 10), but 60 m west of the synclinal axis (near the road) strata are subvertical (Fig. 8). The west limb of the fold dips moderately ~28°W. Two thin, slightly overturned sandstone beds in the head of the arroyo to the east of the hill correlate to the two resistant sandstone beds (#1 and #2) that outline the shape of the syncline in this cross-sectional view. The reconstructed fold pattern (Fig. 10, "reconstructed" because much of the fold has been eroded and some details of the fold are not known, such as whether it had a flat crest) is that of an angular, asymmetric anticline with a steeply dipping front limb on the east, an angular crest, and a longer, moderately dipping back limb on the west. This pattern is similar to beds in the core of the fault-propagation fold shown in the right panel of Figure 5, suggesting that the "Yeso syncline" is a fault-propagation fold (Fig. 10, inset) that formed above a thrust fault with tectonic transport toward the east. However, it differs from the simple, theoretical model in two respects. First, the causative fault is not present in outcrop. Second, the front-limb sandstones (beds #1 and #2) continue into the subsurface and the undeformed beds in front of the anticline would, therefore, be at a lower structural elevation than equivalent strata behind the structure. This observation suggests that the causative fault steps up from a dipping fault-segment rather than a flat

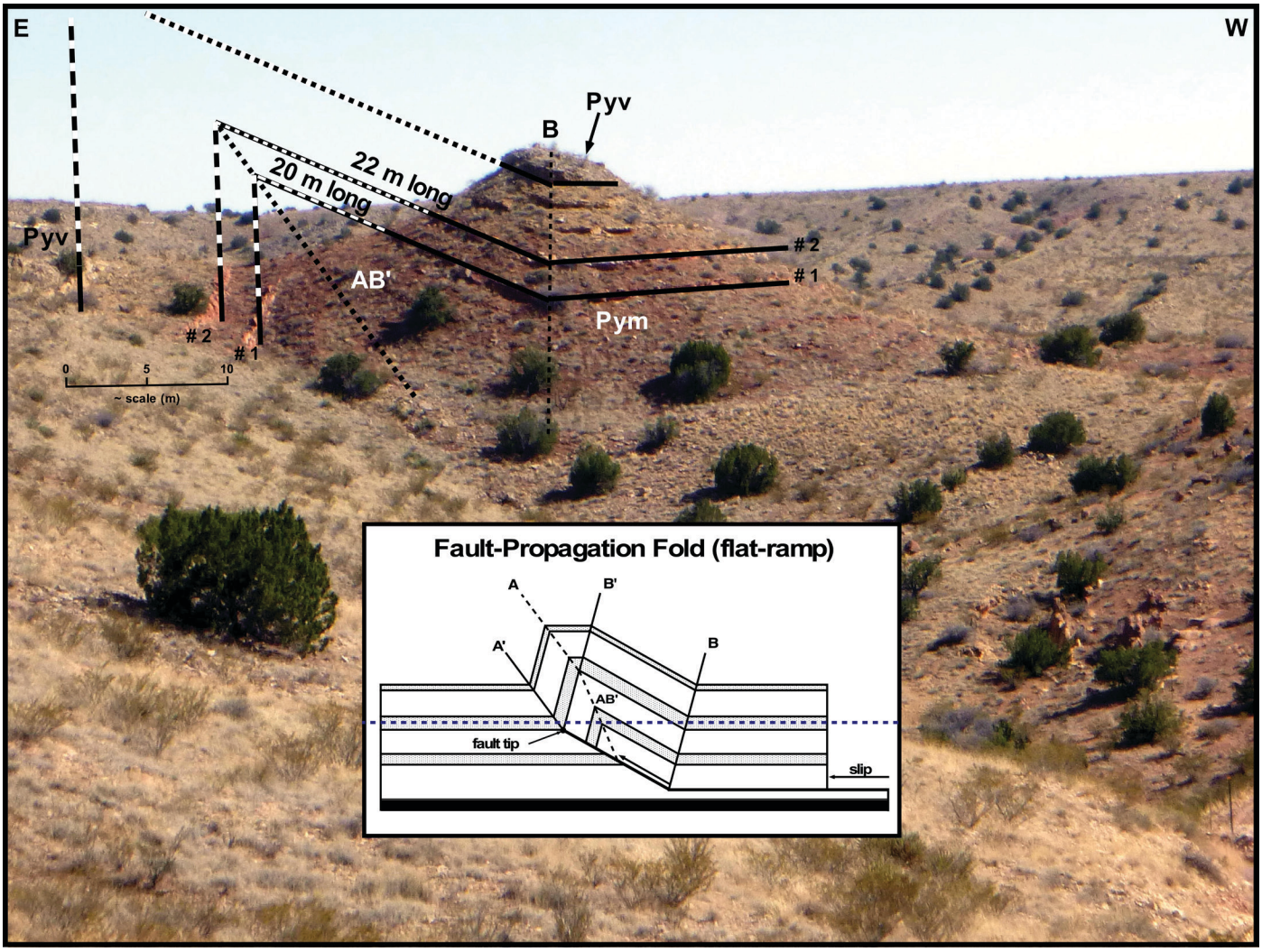

FIGURE 10. Fold #3. Image of the "Yeso syncline," a breached fold (syncline/anticline pair) in an unnamed tributary of Arroyo del Tajo (34.053768°W, -106.773860°N, WGS84). This fold is interpreted as a fault-propagation fold using the generic model shown in the inset. Axial surfaces AB' and B are marked. Solid black lines show bedding attitudes; dashed black and white lines represent eroded parts of the fold. Pyv = the Torres Member of Los Vallos Formation of the Permian Yeso Group; Pym = the Meseta Blanca Formation of the Yeso Group. Blue horizontal line in inset shows that undeformed beds on either side of the model fold are at the same structural elevation. The location of Fold #3 is shown on Figure 8. The "Yeso syncline" is likely one of many small fault-propagation folds east of the broad syncline of the much larger fault-propagation fold represented by Fold #2. Outcrops just right (west) of the image are subvertical strata that are part of the overturned syncline associated with Fold #2. (Photograph courtesy of David Love.)

detachment. Slip on this non-detachment segment would raise strata behind the bend in the fault to a higher structural elevation than those in front of the fold (see Fig. 10 inset). The slightly overturned front limb infers a step-up angle of <25° (Table 2). The amount of slip on the fault cannot be determined reliably from this fragment but is estimated to be between 10 m and 20 m based on the width of the lowest restored back limb (Fig. 10). This is because the ratio of back-limb width to slip of a simple fault-propagation fold is equal to two when the width is measured between parallel axial surfaces B-B' (Fig. 10 inset). When it is measured between nonparallel axial surfaces A-B' and B, the ratio ranges between one and two.

SUMMARY

Reconnaissance analyses of contractional kink folds are presented at three well-exposed outcrops along the Quebradas Back Country Byway, Socorro County, New Mexico. These structures are interpreted to be either fault-bend folds, formed above fault ramps connecting two detachment horizons, or fault-propagation folds formed at the tips of propagating thrust faults. These first-order interpretations were made by comparing the overall shape and limb dips of theoretical folds with the outcrop folds. Adjustments to the fault-shape parameters in the models are discussed that would make better fits with the Quebradas structures.

The small, asymmetric fold exposed in cross section in Permian rocks at the southern end of the Byway (Fold #1) indicates that fault-propagation fold theory is a viable method for interpreting asymmetric folds in the Quebradas region. Here, the fault, fault tip, and fold are displayed at the east end of a north-facing arroyo wall. Features this fold has in common with a generic fault-propagation fold are: (1) a non-planar fault that steps up from a bedding plane detachment; (2) bed offset that decreases to zero at the fault tip; (3) a front synclinal axis that terminates at the fault tip; (4) a fold that is above and in front of a synformal bend in the fault; and (5) a front limb that is steeper than the back limb. It differs from the simple model in having: (1) more than one bend in the fault; (2) more kink bands; and (3) non-horizontal beds in front of and below the ramp likely related to some other strain feature. The multiple bends in the fault produce complexity in the fold. Farther west, a small symmetrical fold that formed above a fault that ramps up to the east at ~29° between two bedding plane detachments indicates that fault-bend folding is also a viable folding mechanism. Elsewhere, in this same outcrop, offset along planar fault segments shows that beds moved rigidly either up or down the fault, but did not form kink bands or drag folds. This rigid-body offset along planar fault segments strongly suggests that deformation along a fault corresponds only to movement above a nonplanar fault.

Similar kink folds or fragments of kink folds are present throughout the structurally complex Quebradas region (see 1:24,000 geologic map citations in introduction and Cather and Axen, in press). The Quebradas folds range from outcrop scale (a few meters across) to subregional scale (a few km). The subregional folds are primarily fault-propagation folds with overturned front limbs that suggest fault step-up angles <25°. The large fold with a highly overturned front limb at Arroyo del Tajo (Fold #2) suggests a fault-propagation fold with a 15° step-up angle. A latterly persistent thrust fault cuts the front limb of this fold (Cather and Colpitts, 2005), indicating that the fold can be modeled as a breakthrough fault-propagation fold. A fault-propagation fold with high-angle breakthrough is offered as a first-order interpretation of the structure; deep erosion of a breakthrough structure provides an internally consistent explanation for a large, isolated overturned syncline present at the southern end of the Quebradas fold belt (Cather and Colpitts, 2005, fig. 1).

ACKNOWLEDGMENTS

We thank Dr. David Love and Mr. Donald Boyd for allowing us to use their outcrop photographs of three folds profiled in this paper. We thank Gary Axen and W. John Nelson for careful and detailed reviews of the paper. Guidebook editor Daniel Koning's comments and suggestions were helpful as well. Their comments improved the paper and helped clarify our thoughts.

REFERENCES

Cather, S.M., 2002 (rev. 2016), Geologic map of the San Antonio 7.5-minute quadrangle, Socorro County, New Mexico: New Mexico Bureau of Geology and Mineral Resources, Open-file Geologic Map 58, scale 1:24,000.

Cather, S.M., and Axen, G.J., in press, Structural geology of the Quebradas region, *in* Cather, S.M., and Koning, D.J., eds., Geology of the Quebradas region, Socorro County, central New Mexico: New Mexico Bureau of Geology and Mineral Resources, Memoir 51.

Cather, S.M., and Colpitts, R.M., Jr., 2005 (rev. 2016), Geologic map of the Loma de las Cañas quadrangle, Socorro County, New Mexico: New Mexico Bureau of Geology and Mineral Resources, Open-file Geologic Map 110, scale 1:24,000.

Cather, S.M., and Koning, D.J., eds., in press, Geology of the Quebradas Region, Socorro County, central New Mexico: New Mexico Bureau of Geology and Mineral Resources, Memoir 51.

Cather, S.M., Colpitts, R.M., Jr., Hook, S.C., and Heizler, M.T., 2004 (rev. 2016), Geologic map of the Mesa del Yeso 7.5-minute quadrangle, Socorro County, New Mexico: New Mexico Bureau of Geology and Mineral Resources, Open-file Geologic Map 92, scale 1:24,000.

Cather, S.M., Osburn, G.R., and Hook, S.C., 2007 (rev. 2016), Geologic map of the Cañon Agua Buena 7.5-minute quadrangle, Socorro County, New Mexico: New Mexico Bureau of Geology and Mineral Resources, Open-file Geologic Map 146, scale 1:24,000.

Cather, S.M., Colpitts, R.M., Jr., Green, M., Axen, G.J., and Flores, S., 2012 (rev. 2016), Geologic map of the Sierra de la Cruz 7.5-minute quadrangle, Socorro County, New Mexico: New Mexico Bureau of Geology and Mineral Resources, Open-file Geologic Map 227, scale 1:24,000.

Cather, S.M., Osburn, G.R., McIntosh, W.C., Heizler, M.T., Hook, S.C., Axen, G.J., Flores, S., and Green, M., 2014 (rev. 2016), Geologic map of the Bustos Well 7.5-minute quadrangle, Socorro County, New Mexico: New Mexico Bureau of Geology and Mineral Resources, Open-file Geologic Map 237, scale 1:24,000.

Dietz, H.M., and McLemore, V.T., this volume, Geochemistry of the Tajo granite, Socorro County, New Mexico: New Mexico Geological Society, Guidebook 72.

Erslev, E.A., 1991, Tri-shear fault-propagation folding: Geology, v. 19, no. 6, p. 617–620.

Koning, D.J., Nelson, W.J., Lucas, S.G., Elrick, S., and Sturgis, L., this volume, Quebradas Region, Day 1 Road Log, from Socorro to Kelly Canyon, Escondida, Loma de las Cañas, and Ojo de Amado: New Mexico Geological Society, Guidebook 72.

Lucas, S.G., Krainer, K., and Colpitts, R.M., Jr., 2005, Abo-Yeso (Lower Permian) stratigraphy in central New Mexico: New Mexico Museum of Natural History and Science, Bulletin 31, p. 101–117.

Lucas, S.G., Krainer, K., Barrick, J.E., Allen, B.D., and Nelson, W.J., this volume (a), Pennsylvanian stratigraphy and biostratigraphy in the Cerros de Amado, Socorro County, New Mexico: New Mexico Geological Society, Guidebook 72.

Lucas, S.G., Krainer, K., and Nelson, W.N., this volume (b), Permian stratigraphy east of Socorro, New Mexico: New Mexico Geological Society, Guidebook 72.

Medwedeff, D.A., and Suppe, J., 1997, Multibend fault-bend folding: Journal of Structural Geology, v. 19, p. 279–292.

Scholle, P.A., 2010, A geologic guide to the Quebradas Back Country Byway: New Mexico Bureau of Geology and Mineral Resources and the Bureau of Land Management, 21 p.

Shaw, J.H., Hook, S.C., and Suppe, J., 1994, Structural trend analysis by axial surface mapping: American Association of Petroleum Geologists, v. 78, no. 5, p. 700–721.

Shaw, J.H., Connors, C., and Suppe, J., 2005, Structural interpretation methods, *in* Shaw, J.H., Connors, C., and Suppe, J., eds., Seismic interpretation of contractional fault-related folds: American Association of Petroleum Geologists, Seismic Atlas, Studies in Geology, v. 53, p. 2–59.

Smith, C.T., Osburn, G.R., Chapin, C.E., Hawley, J.W., Osburn, J.C., Anderson, O.J., Rosen, S.D., Eggleston, T.L., and Cather, S.M., 1983, First-day road log from Socorro to Mesa del Yeso, Joyita Hills, Johnson Hill, Cerros de Amado, Loma de las Cañas, Jornada del Muerto, Carthage, and return to Socorro: New Mexico Geological Society, Guidebook 34, p. 1–28.

Suppe, J., 1983, Geometry and kinematics of fault-bend folding: American Journal of Science, v. 283, p. 648–721.

Suppe, J., 1985, Principles of structural geology: Englewood Cliffs, NJ, Prentice Hall, Inc., 537 p.

Suppe, J., and Medwedeff, D.A., 1990, Geometry and kinematics of fault-propagation folding: Eclogae Geologicae Helvetiae, v. 83, no. 3, p. 409–454.

Tarantula on eolian sand. Photo by Daniel Koning.